Int. J. Electrochem. Sci., 17 **(2022)** Article Number: 221121, doi: 10.20964/2022.11.01

International Journal of
ELECTROCHEMICAL
SCIENCE
www.electrochemsci.org

Comparative Electrochemical Oxidation of Bisphenol A Using BDD, PbO_2, and IrO_2 Anodes: Identification of Active Free Radicals

Hao Li[1,2,*], *Yiqi Du*[2], *Xiaolan Shen*[1,2], *Xinmou Kuang*[1,2], *Jiayi Zhu*[2], *Hairong Wang*[2]

[1] Zhejiang Collaborative Innovation Center for High Value Utilization of Byproducts from Ethylene Project, Ningbo Polytechnic, Ningbo 315800, China
[2] College of Chemical Engineering, Ningbo Polytechnic, Ningbo 315800, China
[*]E-mail: lhkobe@zju.edu.cn

Received: 25 July 2022 / *Accepted:* 27 August 2022 / *Published:* 10 October 2022

The comparative electrochemical oxidation efficiency of bisphenol A (BPA) was explored using boron doped diamond (BDD), PbO_2, and IrO_2 anodes. Several parameters were optimized using the BDD anode. The optimal conditions were a current density of 60 $mA\cdot cm^{-2}$, Na_2SO_4 concentration of 4 $g\cdot L^{-1}$, agitation rate of 600 rpm, and BPA concentration of 50 $mg\cdot L^{-1}$. The BPA removal efficiencies for the BDD, PbO_2, and IrO_2 anodes were 100%, 79.9%, and 19.5%, respectively; only the BDD anode showed complete BPA removal. Similarly, the COD removal efficiencies with the BDD, PbO_2, and IrO_2 anodes were 81.8%, 37.0%, and 6.73%, respectively. Oxidation with the BDD anode was realized mainly by •OH, accounting for approximately 85.6%. In addition, $SO_4{\cdot}^-$ oxidation and direct oxidation accounted for approximately 7.7% and 6.7%, respectively. In the PbO_2 anode, •OH oxidation, $SO_4{\cdot}^-$ oxidation, and direct oxidation accounted for approximately 51.0%, 8.2%, and 40.8%, respectively. In the IrO_2 anode, oxidation was dependent mainly on direct oxidation, and no •OH and $SO_4{\cdot}^-$ were generated.

Keywords: Electrochemical oxidation; BDD; PbO_2; IrO_2; Radicals

1. INTRODUCTION

Electrochemical oxidation technology is used widely in industrial wastewater treatment. Electrochemical oxidation uses electrons as reaction reagents and oxidizes organic pollutants in water through the generation of strong oxidizing active species. This method has a strong oxidation capacity, good treatment effect, high energy efficiency, and strong controllability and does not produce secondary pollution during the treatment process. [1–3] Several factors, such as electrode material, applied current, supporting electrolyte, and solution pH, affect the efficiency of electrochemical oxidation, with the influence of the electrode material being the most significant [4,5]. The electrochemical oxidation reaction is a heterogeneous catalytic reaction on the electrode surface that involves electron transfer. Therefore, the rate of charge transfer determines the reaction rate, which is determined mainly by the electrode potential [6]. Good conductivity, strong corrosion resistance, high mechanical strength, and long service life should characterize electrode materials. Typical electrodes mainly include, among others, metal, metal oxide, and carbon material electrodes [7].

Inert noble metals are often used as materials for metal electrodes, such as Au, Ru, and Pt, which have stable surfaces and high reaction activity [8]. However, the high cost of noble metals significantly limits their large-scale application. Yao et al. used Pt as an anode and Ti as a cathode to realize efficient electrochemical denitrification, with a nitrate removal efficiency of 82.1%, N_2 selectivity of 81.3%, and current efficiency of 63.9% [9]. Experiments have confirmed that anodic oxidation is significant in electrochemical denitrification. However, overall, the oxidation efficiency of metal electrodes remains low. Brillas et al. compared the anodic oxidation of Pt and boron doped diamond (BDD) anodes to treat dopamine hydrochloride solutions, and the results showed a low mineralization rate for the Pt electrode, whereas considerably faster mineralization was acquired using a BDD anode [10].

A metal oxide electrode usually uses a Ti-based coating as a substrate and a layer of metal oxide film deposited on its surface, also known as a dimensionally stable anode electrode. It has high electrocatalytic activity, corrosion resistance, and high stability. In particular, the preparation of an oxide film is controllable [11,12]. Jojoa-Sierra et al. reported that the electrochemical degradation of norfloxacin was realized using IrO_2 as an anode and that the presence of NaCl could substantially improve electrochemical oxidation efficiency [13]. Ajab et al. improved the oxidation activity of the RuO_2 electrode by adjusting the Ru concentration using $RuCl_3$•xH_2O as the coating solution [14]. The RuO_2 electrode had an excellent effect on the degradation of polycyclic aromatic hydrocarbons and chemical oxygen demand (COD) removal when the RuO_2 concentration was 0.8 $mol\cdot L^{-1}$, and the degradation efficiency was improved further by adding a NaCl supporting electrolyte owing to the generated active chlorine and hypochlorite. Wang et al. fabricated a PbO_2/SnO_2 composite anode by doping SnO_2 particles with a PbO_2 film using composite electrodeposition technology to improve the electrocatalytic efficiency of the electrode by improving the active center, oxygen evolution potential, and hydroxyl radical (•OH) generation rate on the electrode surface [15]. Overall, metal oxide electrodes have limited oxidation ability. Hence, it is often necessary to add a supporting electrolyte (mainly NaCl) or prepare a new composite metal electrode to enhance the oxidation ability of metal oxide electrodes.

Carbon materials have good conductivity and a large specific surface area. Graphite [16], carbon nanotube [17], and granular activated carbon [18] are commonly used electrode materials. However, carbon materials also have limitations on their applicability, such as poor stability and easy deactivation. As a unique carbon material, diamond has very high stability. Through boron atom doping, the fabricated BDD electrode shows excellent characteristics, such as a wide potential window, very low background current, high electrochemical stability, corrosion resistance, and low adsorption [19,20]. Recently, the BDD electrode has gained popularity among researchers in wastewater treatment, particularly in removing various refractory organic pollutants. Siedlecka et al. reported the electrochemical oxidation of five anticancer drugs, such as 5-fluorouracil, on the BDD electrode [21]. Zhuo et al. reported the electrochemical oxidation of a perfluorooctane sulfonate substitute using a SnO_2-F-modified BDD anode [22]. Dávila et al. reported the electrochemical oxidation of dibenzothiophenes on the BDD electrode

[23]. These studies all showed high degradation efficiencies and deep removal of pollutants. In particular, the preparation cost of the BDD electrode is relatively high, limiting its large-scale application.

Overall, the electrochemical oxidation efficiencies of different types of electrodes differ significantly owing to different electrochemical oxidation mechanisms. This study mainly investigates the differences in the electrochemical oxidation efficiency of different types of electrodes, mainly inert electrodes (BDD and PbO_2) and an active electrode (IrO_2), and examined the reasons for this by identifying active oxidation species. In this paper, bisphenol A (BPA) wastewater was selected as the target pollutant. BPA, a common plastic product additive in the industry, is a typical persistent organic pollutant that harms the human endocrine and reproductive system [24]. Traditional biochemical wastewater treatment technology cannot remove BPA completely. However, electrochemical oxidation technology based on strong oxidizing species is an efficient method to achieve the complete removal of BPA. The difference in oxidation efficiency can be further highlighted by comparing the degradation of BPA with different anodes.

2. EXPERIMENTAL

2.1. Materials

Condias (Germany) supplied the BDD electrode with double-sized deposited coatings on a niobium plate (20 mm × 20 mm). Yiwanlin Electronic Technology Co., Ltd. (China) supplied the IrO_2 electrode deposited on a titanium plate (20 mm × 20 mm). The PbO_2 electrode deposited on a Ti plate (20 mm × 20 mm) was purchased from Tengerhui Electronic Technology Co., Ltd (China). BPA with a purity exceeding 99% was obtained from Aladdin Industrial Inc., China. All other chemicals were purchased from Aladdin at their analytical grades and used without further purification. All aqueous solutions were prepared with ultrapure water (resistivity > 18 MΩ·cm) at room temperature.

2.2. Electrolysis process

BPA was degraded in batches within an undivided 300 mL electrolytic cell. A magnetic stirrer was used to stir the solution. Each batch contained 200 mL of BPA in the cell, and electrolysis was conducted under galvanostatic conditions using a DC power supply (MS-305D, Maisheng, China). An IrO_2, PbO_2, or BDD electrode was used as the anode, and a same-sized stainless-steel plate was used as the cathode. The distance between the anode and cathode was maintained at 4 cm under all conditions, and the solution was maintained at room temperature.

2.3. Analytical methods

The BPA concentration was determined by UV–vis spectrophotometry (UV-2550, Shimadzu, Japan). The concentration was analyzed quantitatively from the absorption peak area at 275 nm. The

COD value of the solution was determined via rapid digestion spectrophotometry using an intelligent COD rapid analyzer (5B-3C, Lianhua, China). The BPA (COD) removal efficiency was calculated using the following equation:

$$BPA\ (COD)\ removal\ efficiency = \frac{COD_0 - COD_t}{COD_0} \times 100\% \qquad (1)$$

where C_0 and C_t are the concentration of BPA (COD) (mg·L^{-1}) at times $t = 0$ (initial) and t, respectively.

The instantaneous current efficiency (ICE) for the electrochemical oxidation of BPA was derived from the COD value, and can be expressed using the following equation:

$$ICE = \frac{FV(COD_t - COD_{t+\Delta t})}{8I\Delta t} \qquad (2)$$

where F is the Faraday constant (96485 C·mol^{-1}), COD_t and $COD_{t+\Delta t}$ are the COD values (gO_2·L^{-1}) at times t = t and t + Δt, respectively, V is the solution's volume (L), 8 is the oxygen equivalent mass (g·eq^{-1}), I is the applied current (A), and Δt is the degradation time (s).

3. RESULTS AND DISCUSSION

3.1. Effect of investigated parameters on the degradation of BPA at BDD anode

3.1.1. Effect of the current density

Applied current is among the significant factors affecting electrochemical oxidation because the amount of active free radicals produced during electrolysis mainly depends on the applied current [25]. Figure 1 shows the effects of the current density on the degradation efficiency of the BPA solution. When the current density increased from 50 to 70 mA·cm^{-2}, the removal efficiency of BPA increased significantly (Fig. 1a). The complete removal of BPA was realized within 3 h when the current densities were 60 and 70 mA·cm^{-2}. The BPA removal conforms to the pseudo-first-order kinetic model ($\mathrm{Ln}(C_0/C) = k_{obs}t$) (inset in Fig. 1a). When the current densities were 50, 60, and 70 mA·cm^{-2}, the pseudo-first-order degradation rate constant (k_{obs}) values were 0.82, 1.04, and 1.39 h^{-1}, respectively. When the current density increased from 50 to 70 mA·cm^{-2}, the degradation rate increased by 69.5%, confirming that increasing the current density favored the electrochemical oxidation process. The higher degradation of BPA under a higher current density was mainly caused by the accelerated generation of •OH with the higher current [26].

Figure 1b shows the changes in COD removal efficiency during BPA degradation. When the current densities were 50, 60, and 70 mA·cm^{-2}, the COD removal efficiencies after 3 h treatment were 71.5%, 81.8%, and 90.9%, respectively. The COD removal also conformed to the pseudo-first-order kinetics. The corresponding k_{obs} values were 0.40, 0.55, and 0.77 h^{-1}, respectively (inset in Fig. 1b). The degradation rate at a current density of 70 mA·cm^{-2} exceeded that at 50 mA·cm^{-2} by 92.5%, which is higher than the increase in the BPA removal rate, indicating that increasing the current density favored BPA mineralization. However, as the current density increased, some of the applied current was involved with side reactions, such as O_2, H_2O_2, and $S_2O_8^{2-}$ production, which failed to degrade organic pollutants, thereby reducing the current efficiency [27]. Therefore, the change in the ICE value under different current densities was compared (Fig. 1c). The initial ICE value was the largest when the current density was 70 mA·cm^{-2} but decreased dramatically after some time. After approximately 0.5 h of electrolysis, the ICE value was reduced to the minimum of all conditions because of the faster degradation rate and higher pollutant removal rate. As the pollutant concentration in the solution rapidly decreased, the amount of current required to remove the pollutants also decreased, resulting in the current being used mainly for side reactions.

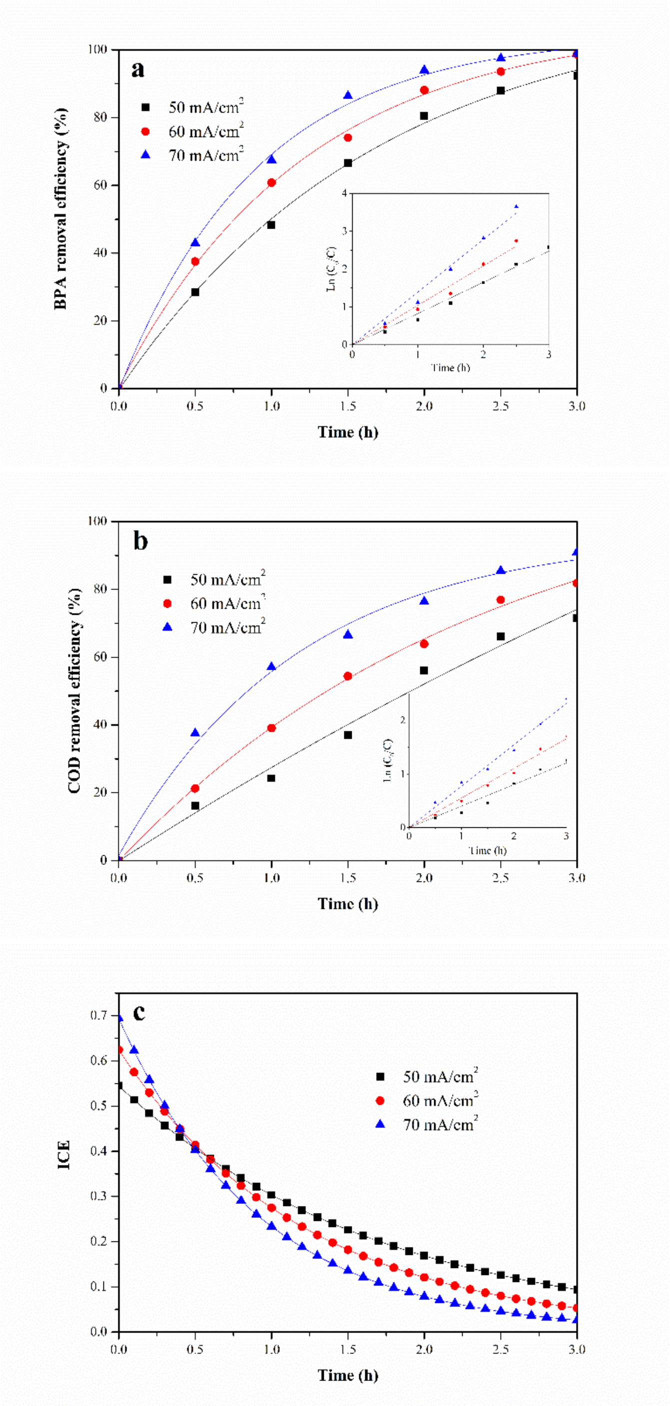

Figure 1. Effect of the current density on the BPA (a) and COD (b) removal efficiencies, and ICE values (c) during the electrochemical oxidation of BPA with a BDD anode. Conditions: BPA concentration of 50 mg·L^{-1}, Na_2SO_4 concentration of 4 g·L^{-1}, and agitation rate of 600 rpm.

3.1.2. Effect of Na_2SO_4

Electrolytes were added in this experiment mainly to enhance the conductivity of the solution, particularly for BPA wastewater with very low conductivity, and to reduce the reaction energy consumption. In this experiment, Na_2SO_4 was selected as the supporting electrolyte; Figure 2 shows its effect on BPA removal. The concentration of Na_2SO_4 slightly affected the BPA removal efficiency, and BPA could be removed completely under all conditions (Fig. 2a). When the Na_2SO_4 concentration were 3, 4, and 5 $g{\cdot}L^{-1}$, the corresponding pseudo-first-order k_{obs} values were similar at 0.97, 1.04, and 1.00 h^{-1}, respectively (inset in Fig. 2a). Figure 2b shows the changes in the COD removal efficiency. The COD removal efficiency was approximately 80% after 3 h of electrolysis under all conditions. The pseudo-first-order k_{obs} values were 0.48, 0.55, and 0.49 h^{-1}, respectively (inset in Fig. 2b); the trend was similar to that of the BPA removal efficiency. The degradation rate was slightly higher when the Na_2SO_4 concentration was 4 $g{\cdot}L^{-1}$. The result was consistent with using the BDD electrode to degrade m-dinitrobenzene reported by Bai et al. [28] This is mainly because in anodic oxidation with the BDD anode, Na_2SO_4 can be oxidized to $S_2O_8^{2-}$ and sulfate radical ($SO_4{\cdot}^{-}$) to promote electrooxidation efficiency. However, excessive Na_2SO_4 will also occupy more active sites on the electrode surface and affect the production of hydroxyl radicals [24,29]. Moreover, the amount of Na_2SO_4 added in this experiment was large, making the effect of its concentration less obvious.

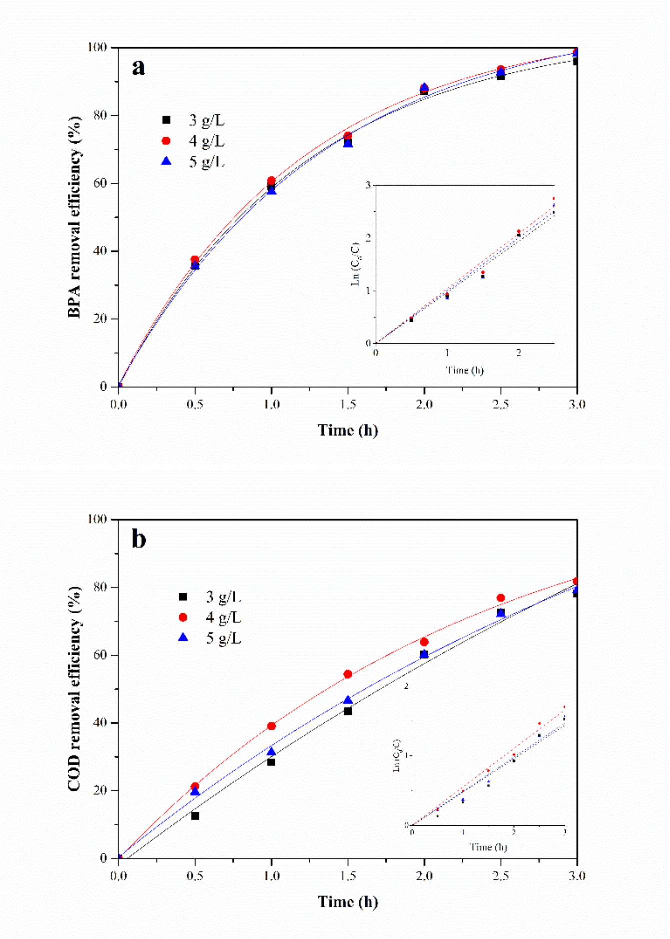

Figure 2. Effect of Na_2SO_4 concentration on the BPA (a) and COD (b) removal efficiencies during the electrochemical oxidation of BPA with a BDD anode. Conditions: BPA concentration of 50 $mg{\cdot}L^{-1}$, current density of 60 $mA{\cdot}cm^{-2}$, and agitation rate of 600 rpm.

3.1.2. Effect of the agitation rate

An electrochemical oxidation reaction is usually an interface reaction. Owing to the short lifetime of free radicals, the pollutants in the solutions need to diffuse to the electrode surface to react with the generated free radicals. The agitation rate is an important factor affecting the diffusion of pollutants in solutions [30]. Figure 3 shows the effects of the agitation rate on BPA degradation. When the agitation rates increased from 400 to 800 rpm, the BPA removal efficiency remained almost constant, with complete removal of BPA achieved in 3 h of electrolysis (Fig. 3a). Furthermore, the corresponding pseudo-first-order k_{obs} values were 0.93, 1.04, and 0.99 h^{-1} when the agitation rates were 400, 600, and 800 rpm, respectively (inset in Fig. 3a). Accordingly, Figure 3b shows the evolution of COD removal efficiency. The result was similar to the BPA removal efficiency. When the agitation rates were 400, 600, and 800 rpm, the pseudo-first-order k_{obs} values were 0.48, 0.55, and 0.51 h^{-1}, respectively (inset in Fig. 3b). The removal rate was relatively fast when the agitation rate was 600 rpm. Too fast and too slow agitation rates were unfavorable to the mass transfer process, causing a slight decrease in the pollutant removal rate. As reported by Peralta et al., the agitation rate did not have a significant effect on the electrolysis of 4-chlorophenol [31]. In this experimental range, the effect of the agitation rate on BPA and COD removal was insignificant, and the optional range of agitation rate was wide.

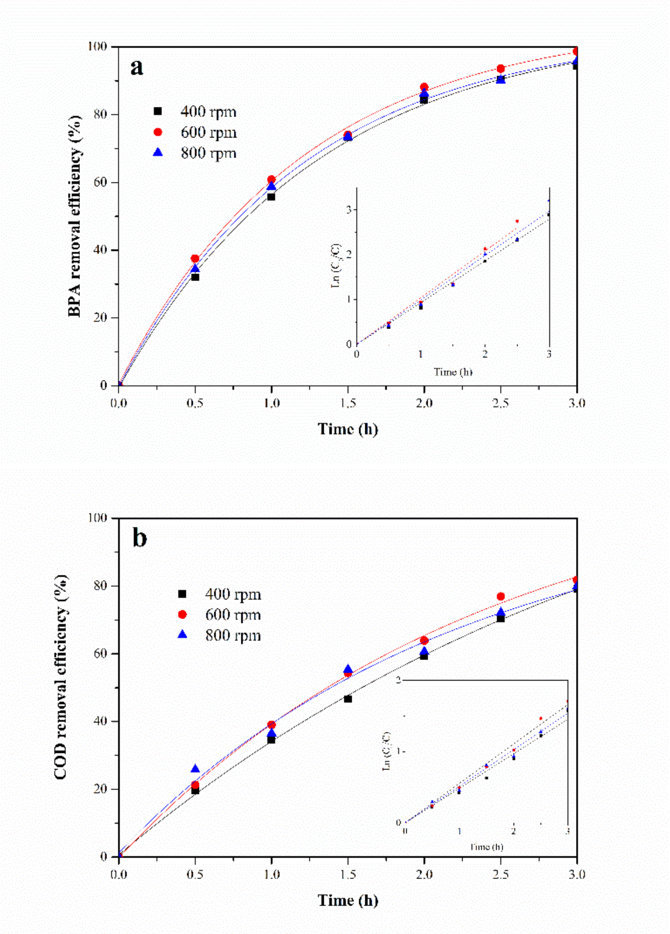

Figure 3. Effect of the agitation rate on the BPA (a) and COD (b) removal efficiencies during the electrochemical oxidation of BPA with a BDD anode. Conditions: BPA concentration of 50 mg·L^{-1}, current density of 60 mA·cm^{-2}, and Na_2SO_4 concentration of 4 g·L^{-1}.

3.1.3. Effect of BPA concentration

Figure 4 shows the effects of the BPA concentration on the electrochemical oxidation of BPA. When the BPA concentrations were 30, 40, and 50 mg·L^{-1}, BPA could be removed completely after 3 h of electrolysis, but its degradation rate decreased gradually (Fig. 4a). The pseudo-first-order k_{obs} values were 1.46, 1.19, and 1.04 h^{-1}, respectively (inset in Fig. 4a). Compared with 30 mg·L^{-1} BPA, the degradation rate decreased by 28.8% when the BPA concentration increased to 50 mg·L^{-1}. Figure 4b shows that the COD removal efficiencies in 3 h of electrolysis were 89.3%, 86.2%, and 81.8% when the BPA concentrations were 30, 40, and 50 mg·L^{-1}, respectively. The pseudo-first-order k_{obs} values were 0.69, 0.63, and 0.55 h^{-1}, respectively (inset in Fig 4b), showing a 20.3% decrease in COD removal rate. This finding is because the generation of active free radicals is mainly dependent on the applied current. The amount of free radicals generated was constant when the current was constant; hence, the degradation rate decreased with increasing pollutant concentration [32]. Although the degradation rate decreased with increasing BPA concentration, the absolute amount of pollutants removed increased, which can be associated with the mass-transfer controlled process at the applied current density [21]. This was confirmed by the evolution of the ICE value (Fig. 4c). When the applied current was constant, the ICE value increased with increasing BPA concentration at any time. Hence, when the BPA concentration was 50 mg·L^{-1}, more current was used for pollutant removal, thereby increasing the absolute amount of pollutant removal. However, when the BPA concentration was 30 mg·L^{-1}, more current was used for side reactions. Salazar et al. reported similar results for the degradation of losartan [33]. The high losartan concentration favored the reaction of •OH with organic compounds, resulting in higher mineralization efficiency.

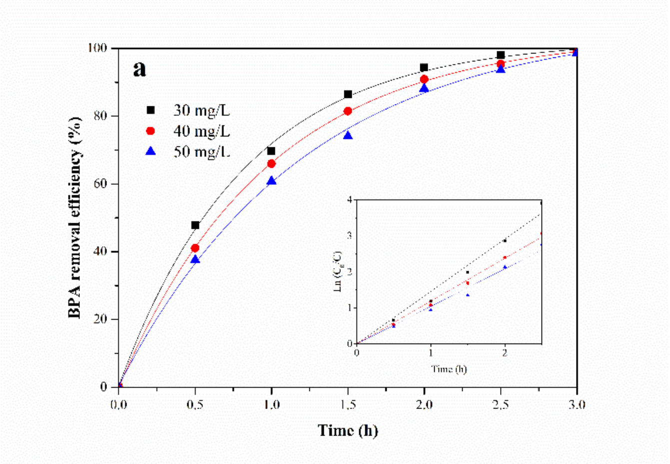

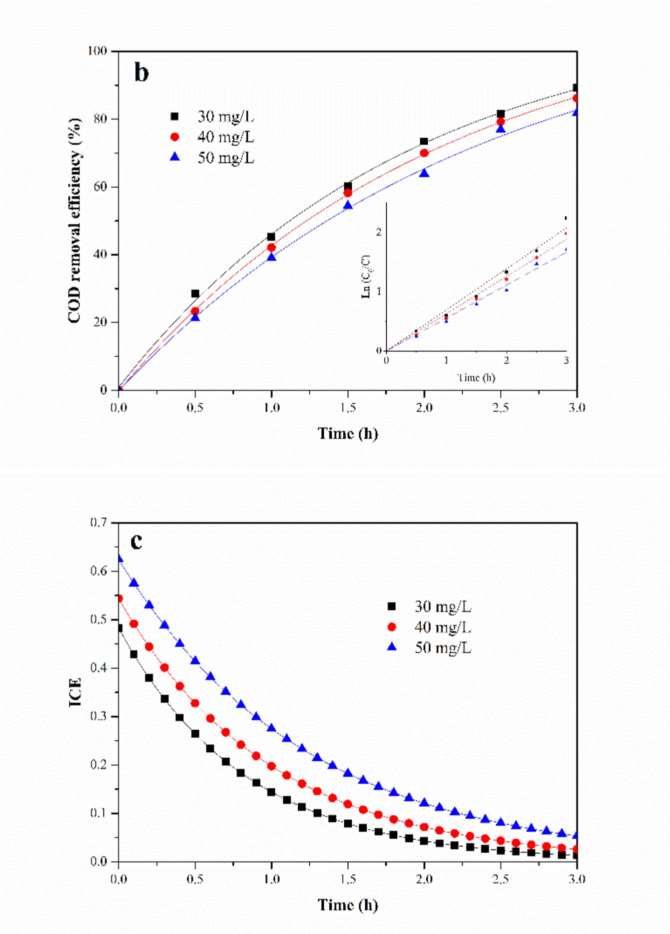

Figure 4. Effect of the BPA concentration on the BPA (a) and COD (b) removal efficiencies, and ICE values (c) during the electrochemical oxidation of BPA with a BDD anode. Conditions: current density of 60 mA·cm^{-2}, Na_2SO_4 concentration of 4 g·L^{-1}, and agitation rate of 600 rpm.

3.1.4. Degradation efficiencies of different anodes

The anode material is a significant factor in electrochemical oxidation and determines the type and quantity of active species produced in the reaction process [34]. In this study, the degradation efficiency of the electrochemical oxidation of BPA by BDD, PbO_2, and IrO_2 was compared, and Figure 5 shows the results. For the BPA removal efficiency (Fig. 5a), complete removal in 3 h of electrolysis could only be achieved using the BDD anode, whereas only 79.9% and 19.5% were achieved using PbO_2 and IrO_2 anodes, respectively. The pseudo-first-order k_{obs} values for the BDD, PbO_2, and IrO_2 anodes were 1.04, 0.49, and 0.073 h^{-1}, respectively (inset in Fig. 5a). The degradation rates of the BDD anode were 2.12 and 14.2 times those of the PbO_2 and IrO_2 anodes, respectively. Furthermore, the mineralization ability of the different electrodes was also investigated, and Figure 5b shows the results. After 3 h of electrolysis, the COD removal efficiencies with BDD, PbO_2, and IrO_2 anodes were 81.8%, 37.0%, and 6.73%, respectively. The corresponding pseudo-first-order k_{obs} values were 0.55, 0.15, and 0.024 h^{-1}, respectively (inset in Fig. 5b). The COD removal efficiencies of the BDD electrode were 3.7 and 22.9 times those of the PbO_2 and IrO_2 electrode, respectively. The BDD electrode had the most significant effect on the removal of both BPA and COD, whereas the IrO_2 electrode had the lowest removal efficiency. Gargouri et al. examined the electrochemical degradation of petroleum hydrocarbons from produced water using PbO_2 and BDD electrodes [35]. The results show that the BDD anode had a higher degradation rate than that on the PbO_2 anode. da Silva et al. compared the degradation of produced water generated by petrochemical industrials using Ti/IrO_2–Ta_2O_5 and BDD anodes; higher TOC and COD removal efficiencies were achieved for the BDD anode under the same operating conditions [36].

In particular, when the BPA degradation and COD removal rates were compared, the difference between the BDD electrode and other electrodes was more obvious in COD removal, indicating that the BDD electrode had stronger mineralization ability. In contrast, the other two electrodes only achieved the transfer of pollutants and had relatively weaker mineralization ability.

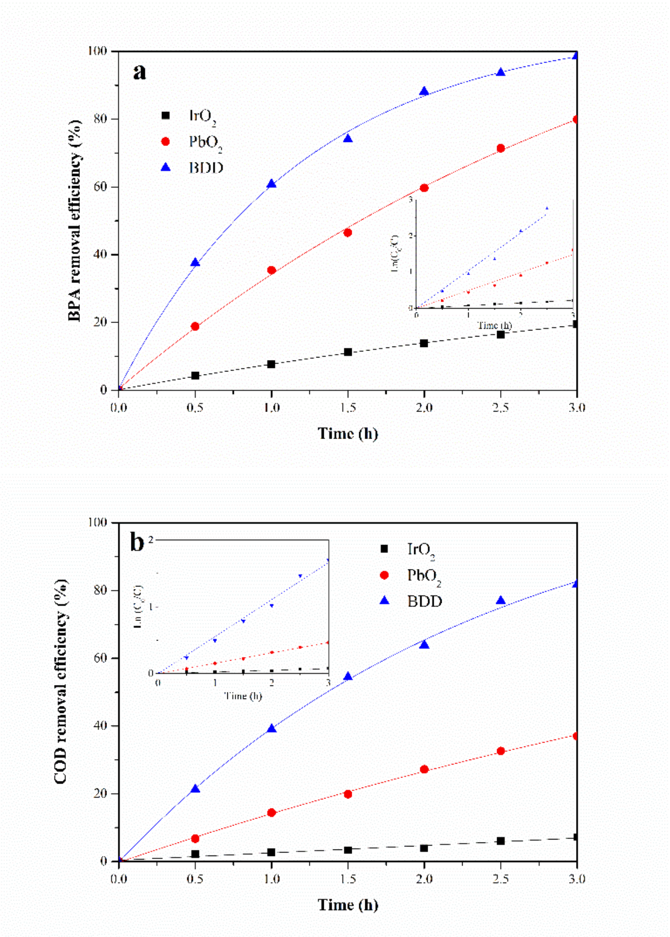

Figure 5. Effect of the anode material on the BPA (a) and COD (b) removal efficiencies during the electrochemical oxidation of BPA. Conditions: BPA concentration of 50 mg·L^{-1}, current density of 60 mA·cm^{-2}, Na_2SO_4 concentration of 4 g·L^{-1}, and agitation rate of 600 rpm.

3.2. Identification of reactive radicals

3.2.1. Reactive radicals in the BDD anode

The difference in the oxidation efficiency of the three electrodes was investigated further by examining the main active free radicals generated during the electrochemical oxidation process using a free radical quenching experiment. Methanol was used to capture both •OH and $SO_4\cdot^-$, and tert-butanol was used to capture •OH [37,38]. Figure 6a shows the effects of the methanol concentration on BPA removal for the BDD electrode. As methanol increased, the BPA removal efficiency decreased significantly. The BPA removal efficiency decreased to only 20.4% when excessive methanol (10 mol·L^{-1}) was added. At this time, the pseudo-first-order k_{obs} value was only 0.070 h^{-1}, which was 6.7% of the degradation rate when no methanol was added (Fig. 6b). The removal of pollutants at this time mainly depended on direct oxidation. Figure 6c shows the effect of tert-butanol concentration on BPA removal. As tert-butanol increased, the removal efficiency of BPA also decreased; however, its inhibition effect was slightly weaker than that of methanol. The removal efficiency of BPA decreased to 36.4% when excessive tert-butanol (5 mol·L^{-1}) was added. At this time, the pseudo-first-order k_{obs} value was 0.15 h^{-1} (Fig. 6d), which was 14.4% of the degradation rate when tert-butanol was not added. The difference in BPA removal by adding methanol and tert-butanol showed that •OH and $SO_4{\cdot}^-$ were generated simultaneously in the oxidation process with the BDD electrode, and their production can be expressed by the following equation [39]:

$$H_2O \rightarrow \cdot OH + H^+ + e^- \tag{3}$$

$$BDD(\cdot OH) + SO_4^{2-} \rightarrow BDD(SO_4^{\cdot -}) + OH^- \tag{4}$$

$$BDD(SO_4^{\cdot -}) + SO_4^{2-} \rightarrow S_2O_8^{2-} + e^- \tag{5}$$

Based on the degradation rate, oxidation with the BDD electrode was realized mainly by •OH, accounting for approximately 85.6%. In addition, the oxidation of $SO_4{\cdot}^-$ accounted for approximately 7.7%; other forms of oxidation, such as direct oxidation, accounted for approximately 6.7%. This is consistent with the results of Song et al. who examined the electrochemical activation of persulfates at the BDD electrode [40]. Even in the presence of persulfate, the degradation of organic pollutants was still dominated by surface adsorbed •OH.

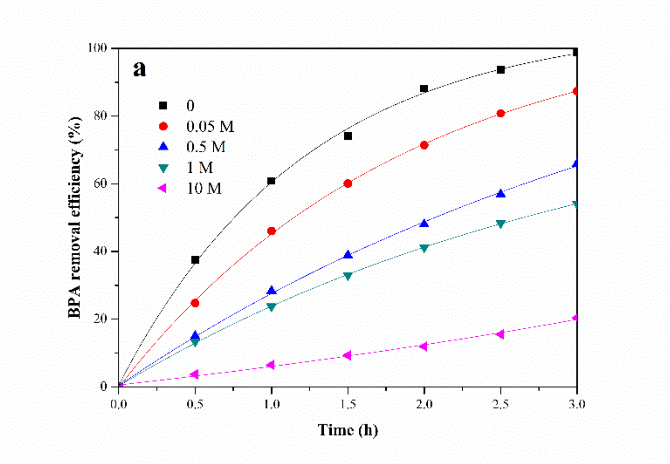

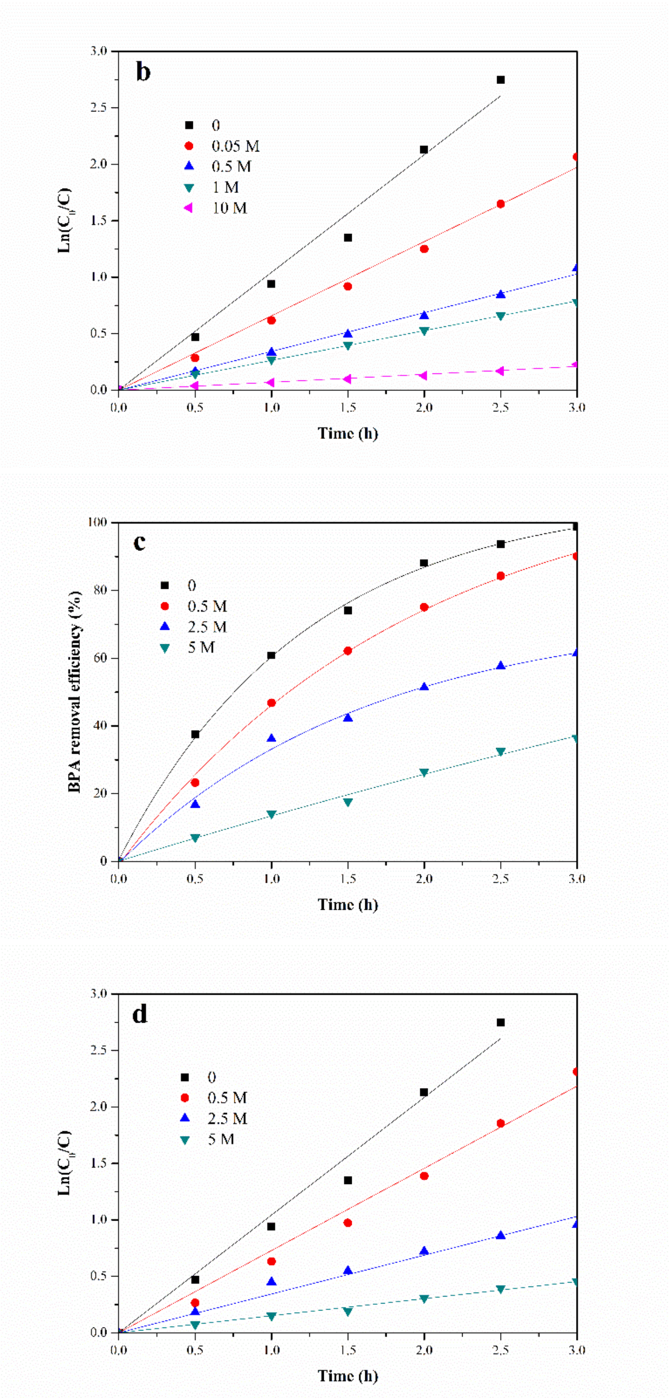

Figure 6. Effect of methanol (a, b) and tert-butanol (c, d) on the BPA removal efficiency during the electrochemical oxidation of BPA with a BDD anode. Conditions: BPA concentration of 50 mg·L^{-1}, current density of 60 mA·cm^{-2}, Na_2SO_4 concentration of 4 g·L^{-1}, and agitation rate of 600 rpm.

3.2.2. Reactive radicals in the PbO_2 anode

The effects of excessive methanol and tert-butanol on the electrochemical oxidation of BPA with a PbO_2 electrode were also investigated; Figure 7a shows the results. When 10 mol·L^{-1} methanol or 5 mol·L^{-1} tert-butanol was added, the BPA removal efficiency decreased to 46.0% or 52.7%, and the corresponding pseudo-first-order k_{obs} values were 0.20 and 0.24 h^{-1}, respectively (inset in Fig. 7a). Compared with the k_{obs} of 0.49 h^{-1} without radical captures, the degradation rates decreased to only 40.8% or 49.0% after addition 10 $mol \cdot L^{-1}$ methanol or 5 $mol \cdot L^{-1}$ tert-butanol, respectively. Similarly, based on the degradation rate, the oxidation of •OH and $SO_4 \cdot^-$ accounted for approximately 51.0% and 8.2%, respectively, whereas the oxidation in the form of direct oxidation accounted for approximately 40.8%. The main active radical generated in the electrochemical oxidation process with the PbO_2 anode was •OH, which was also verified by Zhou et al. in the degradation of pentachlorophenol [41]. However, the amount of •OH generated in the PbO_2 anode was lower than that of the BDD anode because the PbO_2 electrode has a lower oxidation potential than the BDD electrode. The proportion of direct oxidation in the PbO_2 oxidation system was higher, so the overall oxidation efficiency and mineralization ability were lower than those of the BDD electrode.

3.2.3. Reactive radicals in the IrO₂ anode

The effects of excessive methanol and tert-butanol on the electrochemical oxidation of BPA with an IrO_2 electrode were also investigated; Figure 7b shows the results. The BPA removal efficiencies were 18.0% and 18.4% when 10 $mol \cdot L^{-1}$ methanol and 5 $mol \cdot L^{-1}$ tert-butanol, respectively, were added, and the corresponding pseudo-first-order k_{obs} values were 0.068 and 0.067 h^{-1} (inset in Fig. 7b). Compared with the BPA removal efficiency of 19.5% and k_{obs} of 0.073 h^{-1} without radical capture, the degradation efficiency did not show significant changes after addition methanol or tert-butanol, indicating that no active radicals (•OH and $SO_4 \cdot^-$) were generated in the oxidation process with the IrO_2 electrode and that the oxidation was dependent primarily on direct oxidation. Thus, the oxidation ability of the IrO_2 electrode was weak, and both BPA and COD removal efficiencies were low compared to the BDD and PbO_2 electrodes. Borbón et al. studied the electrochemical treatment of dairy wastewater using DSA-type anodes and found that no •OH formed at the DSA surface according to electron spin resonance [42]. Indeed, IrO_2 is a typical active electrode, active free radicals are adsorbed chemically on the electrode surface, and the oxidation is realized mainly by direct electron transfer, whereas the BDD and PbO_2 electrodes are typical inert electrodes, active free radicals are mainly adsorbed physically on the electrode surface, and oxidation is realized in the form of free radicals [43]. The BDD and PbO_2 electrodes showed stronger oxidation efficiency owing to the higher oxidation ability of free radicals.

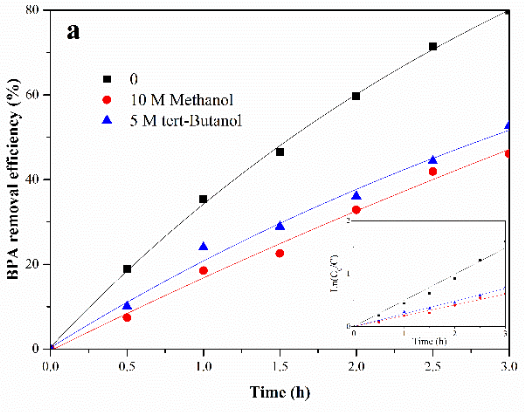

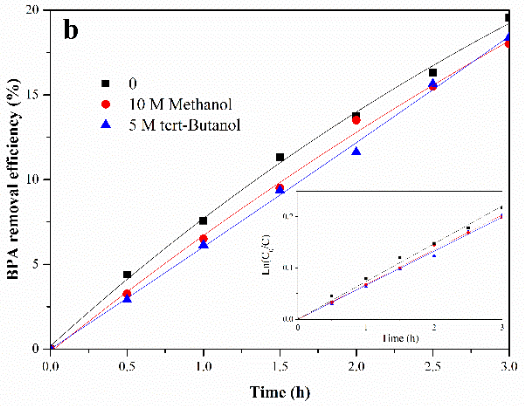

Figure 7. Effect of methanol and tert-butanol on the BPA removal efficiency during the electrochemical oxidation of BPA with PbO_2 (a) and IrO_2 (b) anode. Conditions: BPA concentration of 50 mg·L^{-1}, current density of 60 mA·cm^{-2}, Na_2SO_4 concentration of 4 g·L^{-1}, and agitation rate of 600 rpm.

4. CONCLUSIONS

This study examined the effects of anode materials on BPA electrochemical oxidation. The effects of the applied current density, supporting electrolyte, agitation rate, and BPA concentration were studied and optimized using the BDD anode. The removal efficiencies of both BPA and COD increased significantly when the current density was increased from 50 to 70 mA·cm^{-2}; the complete BPA removal was realized within 3 h. The Na_2SO_4 concentration slightly affected BPA removal. The Na_2SO_4 concentration of 4 g·L^{-1} showed a slightly high degradation rate. The BPA removal efficiency remained almost constant when the agitation rate was increased from 400 to 800 rpm, and the agitation rate of 600 rpm showed a relatively fast degradation rate. When the BPA concentration was increased from 30 to 50 mg·L^{-1}, its degradation efficiency decreased gradually while its ICE value increased, thereby increasing the absolute amount of pollutant removal. Under optimal conditions, the BDD electrode showed the highest degradation and mineralization efficiencies; the BPA and COD removal efficiencies were 100% and 81.8% for BDD, 79.9% and 37.0% for PbO_2, and 19.5% and 6.73% for IrO_2, respectively. Furthermore, identifying the main generated active free radicals was performed through a free radical quenching experiment. Oxidation with the BDD electrode was realized mainly by •OH, accounting for approximately 85.6%, $SO_4{\cdot}^-$ oxidation accounted for approximately 7.7%, and direct oxidation accounted for approximately 6.7%. Oxidation with the PbO_2 electrode was realized mainly by •OH and direct oxidation, which accounted for approximately 51.0% and 40.8%, respectively, whereas the $SO_4{\cdot}^-$ oxidation accounted for only 8.2%. Oxidation with the IrO_2 electrode was dependent mainly on direct oxidation, and no active radicals (•OH and $SO_4{\cdot}^-$) were generated during the oxidation process.

ACKNOWLEDGEMENTS
This work was supported by the Zhejiang Provincial Natural Science Foundation of China (grant number LQ20B070004), and Zhejiang provincial students' scientific and technological innovation activity plan (new talent plan) project (grant number 2022R461A016).

References

1. N. Wang and Q. Zhou, *Int. J. Electrochem. Sci*., 17(2022): 220820.
2. S.O. Ganiyu, C.A. Martínez-Huitle and M.A. Oturan, *Curr. Opin. Electrochem*., 27 (2021) 100678.
3. E. Brillas, *J. Clean. Prod*., 290 (2021) 125841.
4. C. Zhang, Z. Zhang, Z. He and D. Fu, *Electrochim. Acta*, 229 (2017) 55–64.
5. E.J. Martinez, J.G. Rosas, R. Gonzalez, D. Garcia and X. Gomez, *Int. J. Environ. Sci. Technol.*, 15 (2018) 1159.
6. L. Labiadh, A. Barbucci, G. Cerisola, A. Gadri, S. Ammar and M. Panizza, *J. Solid State Electrochem.*, 19 (2015) 3177.
7. Y. Jiang, H. Zhao, J. Liang, L. Yue, T. Li, Y. Luo, Q. Liu, S. Lu, A.M. Asiri, Z. Gong and X. Sun, *Electrochem. Commun*., 123 (2021) 106912.
8. J. Zambrano and B. Min, *Environ. Technol. Innov*., 15 (2019) 100382.
9. J. Yao, Y. Mei, T. Yuan, J. Chen, H. Pan and J. Wang, *J. Electroanal. Chem*., 882 (2021) 115019.
10. E. Brillas, A. Thiam and S. Garcia-Segura, *J. Electroanal. Chem*., 775 (2016) 189.
11. M.C. Medeiros, J.B. de Medeiros, C.A. Martínez-Huitle, T.M.B.F. Oliveira, S.E. Mazzetto, F.F.M. da Silva and S.S.L. Castro, *Sep. Purif. Technol*., 264 (2021) 118425.
12. M.R. Cruz-Díaz, E.P. Rivero, F.A. Rodríguez and R. Domínguez-Bautista, *Electrochim. Acta*, 260 (2018) 726.
13. S.D. Jojoa-Sierra, J. Silva-Agredo, E. Herrera-Calderon and R.A. Torres-Palma, *Sci. Total Environ.*, 575 (2017) 1228.
14. H. Ajab, M.H. Isa and A. Yaqub, *Sustain. Mater. Technol*., 26 (2020) e00225.
15. W. Wang, X. Duan, X. Sui, Q. Wang, F. Xu and L. Chang, *Electrochim. Acta*, 335 (2020) 135649.
16. K. Zhu, X. Wang, X. Ma, Z. Sun and X. Hu, *Electrocatalysis*, 10 (2019) 35–44.
17. B.M. Souza-Chaves, M. Dezotti and C.D. Vecitis, *J. Hazard. Mater*., 382 (2020) 121085.
18. A. Rahmani, M. Leili, A. Seid-mohammadi, A. Shabanloo, A. Ansari, D. Nematollahi and S. Alizadeh, *J. Clean. Prod*., 322 (2021) 129094.
19. D. Clematis and M. Panizza, *Curr. Opin. Electrochem*., 30 (2021) 100844.
20. M. Ghazouani, H. Akrout and L. Bousselmi, *Desalin. Water Treat.*, 53 (2015) 1107.
21. E.M. Siedlecka, A. Ofiarska, A.F. Borzyszkowska, A. Białk-Bielińska, P. Stepnowski and A. Pieczyńska, *Water Res*., 144 (2018) 235.
22. Q. Zhuo, J. Wang, J. Niu, B. Yang and Y. Yang, *Chem. Eng. J.*, 379 (2020) 122280.
23. O.O. Dávila, L.L. Bergeron, P.R. Gutiérrez, M.M.D. Jiménez, I. Sirés, E. Brillas, A.F.R. Navarro, J.B. Arandes and J.V.S. Llopis, *J. Electroanal. Chem*., 847 (2019) 113172.
24. R.C. Burgos-Castillo, I. Sirés, M. Sillanpää and E. Brillas, *Chemosphere*, 194 (2018) 812.
25. M.F. García-Montoya, S. Gutiérrez-Granados, A. Alatorre-Ordaz, R. Galindo, R. Ornelas and J.M. Peralta-Hernández, *J. Ind. Eng. Chem*., 31 (2015) 238.
26. V. Kandavelu, S. Yoshihara, M. Kumaravel and M. Murugananthan, *Diam. Relat. Mater*., 69 (2016) 152.
27. S.M.L. de Oliveira Marcionilio, G.M. Alves, R.B. Góes e Silva, P.J. Lima Marques, P.D. Maia, B.A.D. Neto and J.J. Linares, *Environ. Sci. Pollut. Res*., 23 (2016) 19084.
28. H. Bai, P. He, J. Pan, J. Chen, Y. Chen, F. Dong and H. Li, *J. Colloid. Interface. Sci.*, 497 (2017) 422.
29. Z. Chen, S. Geng, J. Xiao, F. Zhao, K. Wang, Y. Wang, P. Tsiakaras and S. Song, *Chem. Eng. J.*, 431 (2022) 134332.
30. S.M.L. de Oliveira Marcionilio, R. Crisafulli, G.A. Medeiros, M. de S. Tonha, J. Garnier, B.A.D. Neto and J.J. Linares, *Chemosphere*, 224 (2019) 343.
31. E. Peralta, M. Ruíz, G. Martínez, J. Mentado-Morales, L.G. Zárate, M.E. Cordero, M.A. Garcia-Morales, R. Natividad and A. Regalado-Méndez, *Int. J. Electrochem. Sci*., 13 (2018) 4625.
32. R. Ennouri, M. Kchaw, M. Panizza and S.C. Elaoud, *J. Electrochem. Soc.*, 164 (2017) E213.

33. C. Salazar, N. Contreras, H.D. Mansilla, J. Yáñez and R. Salazar, *J. Hazard. Mater.*, 319 (2016) 84.
34. N. Klidi, D. Clematis, M. Delucchi, A. Gadri, S. Ammar and M. Panizza, *J. Electroanal. Chem.*, 815 (2018) 16.
35. B. Gargouri, O.D. Gargouri, B. Gargouri, S.K. Trabelsi, R. Abdelhedi and M. Bouaziz, *Chemosphere*, 117 (2014) 309.
36. A.J.C. da Silva, E.V. dos Santos, C.C. de Oliveira Morais, C.A. Martínez-Huitle and S.S.L. Castro, *Chem. Eng. J.*, 233 (2013) 47.
37. J. Cai, M. Zhou, X. Du and X. Xu, *Sep. Purif. Technol.*, 254 (2021) 117560.
38. S.O. Ganiyu and M.G. El-Din, *Appl. Catal. B Environ.*, 279 (2020) 119366.
39. F. Escalona-Durán, D.R. da Silva, C.A. Martínez-Huitle and P. Villegas-Guzman, *Chemosphere*, 253 (2020) 126599.
40. H. Song, L. Yan, J. Jiang, J. Ma, Z. Zhang, J. Zhang, P. Liu and T. Yang, *Water Res.*, 128 (2018) 393.
41. Y. Zhou, M. Cui, Y. Ren, Y. Lee, J. Ma, Z. Han and J. Khim, *Chemosphere*, 306 (2022) 135547.
42. B. Borbón, M.T. Oropeza-Guzman, E. Brillas and I. Sirés, *Environ. Sci. Pollut. Res.*, 21 (2014) 8573.
43. A. Karaçali, M. Muñoz-Morales, S. Kalkan, B.K. Körbahti, C. Saez, P. Cañizares and M.A. Rodrigo, *Chemosphere*, 225 (2019) 19.